AERODYNAMICS ANALYSIS of NREL S809 HORIZONTAL AXIS WIND TURBINE USING ANSYS/FLUENT

S.Karthik
Assistant Professor/Department of Mechanical Engineering, P.S.N.A College of Engineering & Technology, Dindigul, Tamilnadu, India
E-mail: karthiksmp@gmail.com.

Abstract

Currently research has concentrated on improving the aerodynamic performance of wind turbine blade through wind tunnel testing and theoretical studies. These efforts are much time consuming and need expensive laboratory resources. However, wind turbine simulation through Computational Fluid Dynamics (CFD) software offers inexpensive solutions to aerodynamic blade analysis problem. In this work, two-dimensional airfoil CFD models are presented using ANSYS-FLUENT software. The dimensionless lift, drag and pitching moment coefficients were calculated for wind turbine. Then various values of lift coefficient are determined for various angles of attack. Then the optimal angle of attack for which lift coefficient is maximum is determined. Simulation is done for both laminar and turbulent flow.

1. INTRODUCTION:

Wind energy is an abundant resource in comparison with other renewable resources. Moreover, unlike the solar energy, the utilization could not be affected by the climate and weather. Wind turbine was invented by engineers in order to extract energy from the wind. Because the energy in the wind is converted to electric energy, the machine is also called wind generator. Figure 1-1 shows the growth rate of wind generator capacities, which has increased significantly in the last ten years. The total installed capacity of wind power generators was 159,213 MW at the end of 2009 (World Wind Energy Report 2009).

A wind turbine consists of several main parts, i.e. the rotor, generator, driven chain, control system and so on. The rotor is driven by the wind and rotates at predefined speed in terms of the wind speed, so that the generator can produce electric energy output under the regulation of the control system. In order to extract the maximum kinetic energy from wind, researchers put much effort on the design of effective blade geometry. In the early stage, the aero foils of helicopters were used for wind turbine blade design, but now, many specialized aero foils have been invented and used for wind turbine blade design. Moreover, a rotor blade may have different aero foils in different sections in order to improve the efficiency, so the modern blades are more complicated and efficient comparing to early wind turbine blades.

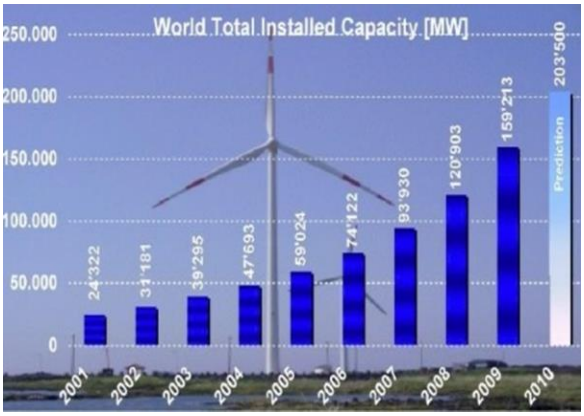

Figure 1-1 World total installed capacity

In the early stage, the research on wind turbine blade design was limited on theoretical study, field testing and wind tunnel testing which need a lot of efforts and resources. Due to the development of computer aided design codes, they provide another way to design and analyse the wind turbine blades. Aerodynamic performance of wind turbine blades can be analyzed using computational fluid dynamics (CFD), which is one of the branches of fluid mechanics that uses numerical methods and algorithms to solve and analyze problems of fluid flows. Meanwhile, finite element method (FEM) can be used for the blade structure analysis. Comparing to traditional theoretical and experimental methods,

numerical method saves money and time for the performance analysis and optimal design of wind turbine blades.

2. LITERATURE REIVIEW

In the past few years, many studies have been focused on wind turbine simulation through Computational Fluid Dynamics (CFD) software offers inexpensive solutions to aerodynamic blade analysis problem.

Chris kaminsky, et al [1] A CFD study of Wind Turbine Aerodynamics, to analyze the effectiveness of VAWT and aerodynamics of various geometry different physical settings

Han Cao, et al [2] Aerodynamics Analysis of Small Horizontal Axis Wind Turbine Blades by Using 2D and 3D CFD Modeling in their work Aerodynamics behavior of HAWT for various angle of attack were analyzed using ansys and analysis of wake effect and noise were carried out.

Muhammad I.H.B.Z. Abidin, et al [3] CFD analysis of miniature Wind Turbine. This work Comparative study has been conducted so that the result from BEM theory and CFD analysis.

David Hartwanger, et al, [4] carried 3D modeling of wind turbine using CFD. This work they made 3D results is used to modify the classical actuator disk treatment of wind turbine

Dayanesh A. Digraskar, et al,[5] Simulation of flow over Wind Turbines, in this research Aerodynamics analysis of HAWT and code is generated to test on locally modeled wind turbine.

Walter P. Wolfe, Stuart S. Ochs, et al [6] CFD Calculations of S809 Aerodynamic Characteristics. Work carried on Comparison of aerodynamics coefficient with wind tunnel data's was made.

3. COMPUTATIONAL FLUID DYNAMICS (CFD)

With Computational Fluid Dynamics we indicate the numerical solution of the differential governing equations of fluid flows, with the help of computers. This technique has a wide range of engineering applications. In the field of aerodynamic research this technique has become increasingly important and it is prominent for studying turbo machinery.

A number of valuable advantages are achieved following a CFD approach to a fluid dynamic problem:

- CFD is faster and definitely cheaper. A considerable reduction of time and costs for solving the problems is offered compared to the traditional approaches. A conscious assessment of different solutions is available in the early phase of the design process, in order to fit with the requested tasks. Thus, experimental tests would be done just on few models, resulted from the CFD analysis.
- Full-size analysis is hard to perform for large systems, like modern wind turbines are, or for extreme thermo-flow conditions as well as narrow geometries. A CFD study is a favourable choice in these cases.
- A key–important quality of CFD are the detailed solutions allowed by the recent techniques (and computer technologies), even for time-dependent flows and complex systems.
- The numerical models of the physical problems have good accuracy and reliability, due again to the newest mathematical improvements of solution schemes and of turbulence models.
- Due to the last two advances, in most of the cases the prediction of a fluid dynamic problem does not require a dedicated powerful workstation and sometimes a personal computer might be sufficient.

The numerical modelling of a fluid dynamics problem implicates first a precise reading of the physical phenomena. All the relevant features of interest should be indicated at that first step, including geometry, materials, boundary conditions, to be defined in the simplest way, but without introducing extreme errors with the hypothesis. Nevertheless, a number of simplifications is always

accepted, and is inevitable in order to model properly fluid dynamics problems.

3.1 THE STRUCTURE OF CFD CODE

In commercial codes friendly interfaces gives the user the possibility of easy setting the various options and analyze the results. Three large parts are generally indicated of a CFD code, which correspond to three phases of the problem analysis:

1. Preprocessor
2. Solver
3. Post-processing

3.2 THE STRATEGY OF CFD

Broadly, the strategy of CFD is to replace the continuous problem domain with a discrete domain using a grid. In the continuous domain, each flow variable is defined at every point in the domain. For instance, the pressure p in the continuous 1D domain shown in the figure below would be given as $p = p(x), 0 < x < 1$

In the discrete domain, each flow variable is defined only at the grid points. So, in the discrete domain shown below, the pressure would be defined only at the N grid points.

$$p_i = p(x_i), \quad i = 1, 2, \ldots, N$$

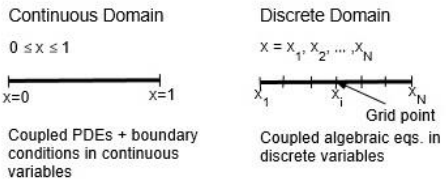

In a CFD solution, one would directly solve for the relevant flow variables only at the grid points. The values at other locations are determined by interpolating the values at the grid points.

The governing partial differential equations and boundary conditions are defined in terms of the continuous variables p, V ⃗ etc. One can approximate these in the discrete domain in terms of the discrete variables pi, V ⃗i·etc. The discrete system is a large set of coupled, algebraic equations in the discrete variables. Setting up the discrete system and solving it (which is a matrix inversion problem) involves a very large number of repetitive calculations, a task we humans palm over to the digital computer.

This idea can be extended to any general problem domain. The following figure shows the grid used for solving the flow over an airfoil. We'll take a closer look at this airfoil grid soon while discussing the finite-volume method.

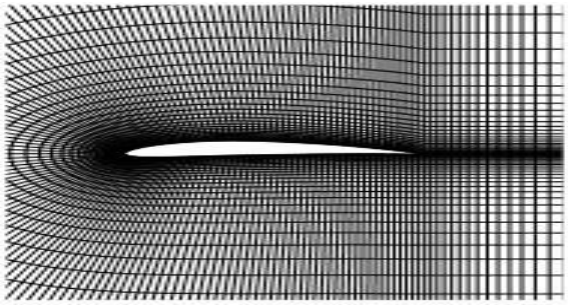

3.3 DISCRITIZATION USING FINITE VOLUME METHOD

If you look closely at the airfoil grid shown earlier, you'll see that it consists of quadrilaterals. In the finite-volume method, such a quadrilateral is commonly referred to as a "cell" and a grid point as a "node". In 2D, one could also have triangular cells. In 3D, cells are usually hexahedral, tetrahedral, or prisms. In the finite-volume approach, the integral form of the conservation equations are applied to the control volume defined by a cell to get the discrete equations for the cell. The integral form of the continuity equation for steady, incompressible flow is

$$\int_S \vec{\mathbf{V}} \cdot \hat{\mathbf{n}}\, dS = 0$$

The integration is over the surface S of the control volume and ˆ n is the outward normal at the surface. Physically, this equation means that the net volume flow into the control volume is zero.

Consider the rectangular cell shown below.

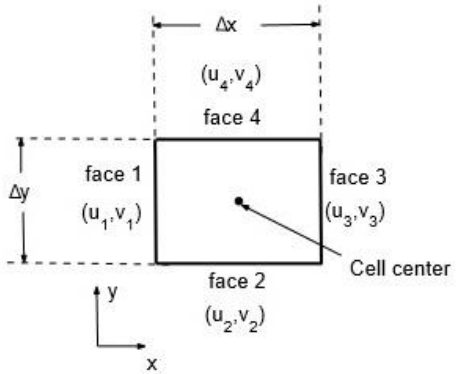

The velocity at face i is taken to be $\vec{V}_i = u_i \vec{i} + v_i \vec{j}$. Applying the mass conservation equation to the control volume defined by the cell gives

$$-u1\Delta y - v2\Delta x + u3\Delta y + v4\Delta x = 0$$

This is the discrete form of the continuity equation for the cell. It is equivalent to summing up the net mass flow into the control volume and setting it to zero. So it ensures that the net mass flow into the cell is zero i.e. that mass is conserved for the cell. Usually, though not always, the values at the cell centers are solved for directly by inverting the discrete system. The face values u1, v2, etc. are obtained by suitably interpolating the cell-center values at adjacent cells.

Similarly, one can obtain discrete equations for the conservation of momentum and energy for the cell. One can readily extend these ideas to any general cell shape in 2D or 3D and any conservation equation. Take a few minutes to contrast the discretization in the finite-volume approach to that in the finite-difference method discussed earlier.

Look back at the airfoil grid. When you are using FLUENT, it's useful to remind yourself that the code is finding a solution such that mass, momentum, energy and other relevant quantities are being conserved for each cell. Also, the code directly solves for values of the flow variables at the cell centers; values at other locations are obtained by suitable interpolation.

3.4 THE PRINCIPLE THEORIES RELEVANT TO CFD MODELLING

No matter what kind of CFD software is, the main processes of simulation are the same. Setting up governing equations is the precondition of CFD modeling; mass, momentum and energy conservation equation are the three basis governing equations. After that, Boundary conditions are decided as different flow conditions and a mesh is created. The purpose of meshing model is discretized equations and boundary conditions into a single grid. A cell is the basic element in structured and unstructured grid. The basic elements of two-dimensional unstructured grid are triangular and quadrilateral cell. Meanwhile, the rectangular cell is commonly used in structured grid. In three-dimensional simulation, tetrahedra and pentahedra cells are commonly used unstructured grid and hexahedra cell is used in structured grids. The mesh quality is a prerequisite for obtaining the reasonably physical solutions and it is a function of the skill of the simulation engineer. The more nodes resident in the mesh, the greater the computational time to solve the aerodynamic problem concerned, therefore creating an efficient mesh is indispensable. Three numerical methods can be used to discretize equations which are Finite Different Method (FDM), Finite Element Method (FEM) and Finite Volume Method (FVM). FVM is widely used in CFD software such as Fluent, CFX, PHOENICS and STAR-CD, to name just a few. Compared with FDM, the advantages of the FVM and FEM are that they are easily formulated to allow for unstructured meshes and have a great flexibility so that can apply to a variety of geometries

3.5 THE SOFTWARE FLUENT

3.5.1 FINITE-VOLUME APPROACH

The commercial code Fluent solve the governing integral equations for the conservation of mass and momentum, and (when appropriate) for energy and other scalars, such as turbulence and chemical species. In both cases a control-volume-based technique is used, which consists of:

- Division of the domain into discrete control volumes using a computational grid.
- Integration of the governing equations on the individual control volumes to construct algebraic equations for the discrete dependent variables (un- known), such as velocities, pressure, temperature, and conserved scalars.
- Linearization of the discretized equations and solution of the resultant linear equation system, to yield updated values of the dependent vari-ables.

Fluent is a commercial 2D/3D unstructured mesh solver, which adopts multigrid solution algorithms. It uses a co-located grid, meaning that all flow parameters are stored in the cell-centers. It is written in C-language, which allows users to introduce a number of model modification through UDFs. Pro- cases can be easily parallelized on multiple computer nodes.

Two numerical methods are available in Fluent:

- Pressure-based solver
- Density-based solver

The first one was developed for low-speed incompressible flows, whereas the second was created for the high-speed compressible flows solution. Although they have been recently modified in order to operate for a wider range of flow conditions, in the present study, which involves incompressible flows, the pressure-based approach was preferred.

3.5.2 DEFINING BOUNDARY CONDITIONS

Boundary conditions (BCs) specify the flow variables on the boundaries of the chosen physical model. They are therefore a critical component of a simulation, and it is important they are specified appropriately.

1. Wall (no-slip)

Wall BC are used to bound fluid and solid regions, for instance the blade surface in a wind turbine model. The no-slip condition is the default setting for viscous flows and the shear-stress calculation in turbulent flows follows the adopted turbulent model.

2. Wall (Euler)

Instead of the no-slip condition, a ideal-slip or Euler-slip can be specified, which might be useful to limit the influence from artificial boundaries too close to the model, e.g. the computational domain shell.

3. Velocity-Inlet

Velocity inlet boundary conditions are used to define the flow velocity, along with all relevant scalar properties of the flow, at flow inlets. This BC is suitable for incompressible flows, whereas for compressible flows ill lead to a non-physical result because stagnation conditions are floating. It is possible so set both constant and variable parameters, as well as they can be alternatively uniform or non-uniformly distributed along the boundary itself.

4. Pressure-Outlet

It means that a specific static pressure at outlet is set, and allows also a set of backflow conditions to minimize convergence difficulties. The radial equilibrium distribution is also added for rotating domain simulations, so that pressure gradient is given as a function of the distance from the axis of rotation r and the tangential velocity component $v\theta$.

5. Symmetry

It is the analogous of a zero-shear slip wall in viscous flow. Zero normal velocity is at a symmetry plane and zero normal gradients of all variables exist there as well.

6. Periodic

They are used to take advantage from the periodically repeating nature of both the geometries and flow patterns. Periodic boundaries are always in pair and the overlooking volumes on the two surface are direct neighbors, i.e. the out coming flow from one, the incoming flow is into the other.

3.6 SOLUTIONS METHODS

- Standard k−ε model: it has a nice stability and precision for high Reynolds number turbulent flow but it is not suitable for some simulation with rotational effect.
- RNG k−ε model: it can used for low Reynolds number flow, as considering the rotational effect, the simulated accuracy will be enhanced in rapidly strain flow.
- Realizable k−ε model: it is more accurate for predicting the speeding rate of both planar and round jets but it will produces non-physical turbulent viscosities when the simulated model includes both rotating and stationary fluid zone.
- Standard k-ω model: it contains the low-Reynolds-number effects, compressibility and shear flow spreading. It has a good agreement with measurements with problems of far wake, mixing layers and plane, round, and radial jets.
- Shear-stress transport (SST) k-ω model: because it absorbs both the property of good accuracy in the near-wall region of standard k-ω model and nice precision in the far field region of k−ε model, it is more accurate and reliable for a wider class flow than the standard k-ω model.
- Reynolds stress model: Abandoning the eddy-viscosity hypothesis, the Reynolds stress model (RSM) calculates the Reynolds stresses directly. Theatrically, it is much more accurate than k−ε and k-ω model, but five additional transport equations in 2D flows and seven additional transport equations in 3D flows seize huge resources in computer and a long simulated time.

3.7 HAWT CFD MODELLING OBJECTIVES

Nowadays, CFD modeling has been widely used in wind turbine analysis. In 2D modeling, it can

be used to evaluate the lift, drag and moment value and estimate the separation point.

Try to achieve an accurate lift, drag and momentum coefficient during aero foil simulation is the one of the objectives. The critical angle of attack is defined as an angle which can produce maximum lift, above the critical angle of attack, a stall condition occurs as air flow becomes fully separated. This means that when angle of attack increases further, wind turbine blade will get into fully stalled regime. When wind turbine blades are working on the stall condition, noise will be increased significantly and wind turbine vibration may happen. It is valuable to investigate the critical angle of attack, because, in principle, change the blade pitch angle to the so-called critical aerodynamic angle of attack leads the aero foil into fully stalled position so that limits the aerodynamic power output.

4. AEROFOIL MODELING AND AERODYNAMICS ANALYSIS

4.1 Two-dimensional aero foil modeling

A simulation model can be created in CATIA directly or imported from other CAD software packages,

Such as Solid Works and Pro/Engineer. In this section, aero foil NREL S809 is modeled.

4.2 NREL S809 modeling

Figure 4-1 is the profile of NREL S809 airfoil. We use unstructured triangular meshing methods for the Modeling the NREL S809. Here the length of computational domain show in fig. 4-3 for the unstructured grid was 29.5 times that of chord length and width was 25 times the chord length. The mesh consists of 3808 triangular cells. By using identical boundary and computational conditions, the pressure and velocity distributions were obtained by the software.

The standard coordinates has been used to draw the aero foil provided by National Renewable Energy laboratory shown in table below. The aerofoil drawn from this data are shown in figure 4-2.

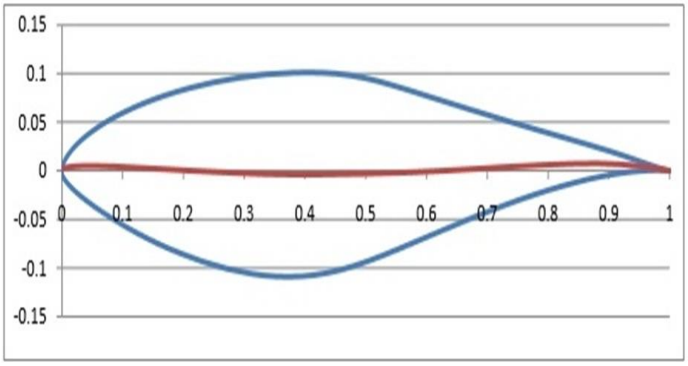

Figure 4-1 The profile of NREL S809

x/c	y/c	x/c	y/c	x/c	y/c
1.000000	0.000000	0.519832	0.093268	0.395329	-0.108011
0.996203	0.000487	0.474243	0.099392	0.481920	-0.097347
0.985190	0.002373	0.428461	0.101760	0.527928	-0.086571
0.967844	0.005960	0.382612	0.101840	0.676744	-0.047441
0.945073	0.011024	0.337260	0.100070	0.727211	-0.035100
0.917488	0.017033	0.292970	0.096703	0.776432	-0.024204
0.885293	0.023458	0.250247	0.091908	0.823285	-0.015163
0.848455	0.030280	0.209576	0.085851	0.866630	-0.008204
0.807470	0.807470	0.171409	0.078687	0.905365	-0.003363
0.763042	0.045974	0.136174	0.070580	0.938474	-0.000487
0.715952	0.054872	0.104263	0.052224	0.965086	0.000743
0.667064	0.064353	0.076035	0.042352	0.984478	0.000775
0.617331	0.074214	0.031910	0.032299	0.996141	0.000290
0.567830	0.084095	0.016590	0.022290	1.000000	0.000000

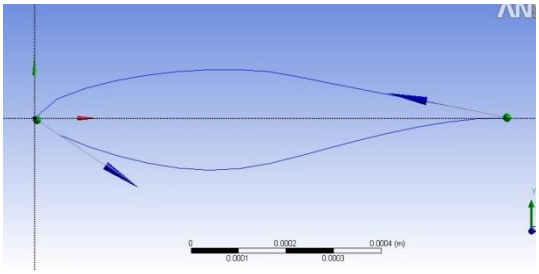

Figure 4-2 The profile of NREL S809 using CATIA

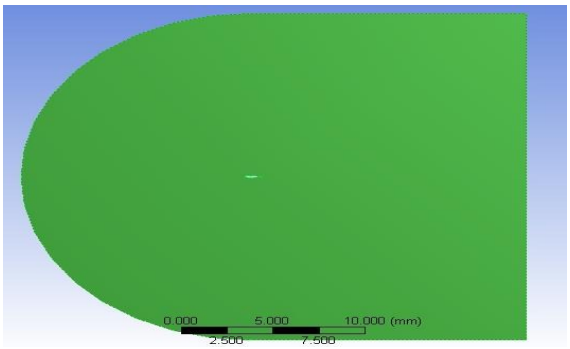

Figure 4-3 Computational Domain of NREL S09 by using Unstructured grid

A large number of grids around the aero foil surface is used to capture the pressure gradient accurately at the boundary layer. This is because the adverse pressure gradient induces flow separation. Stall will occur when separation region extends. In the far-field area, the mesh resolution can become progressively coarser since the flow gradients approach zero. The meshing overview is shown in Figure 4-4.

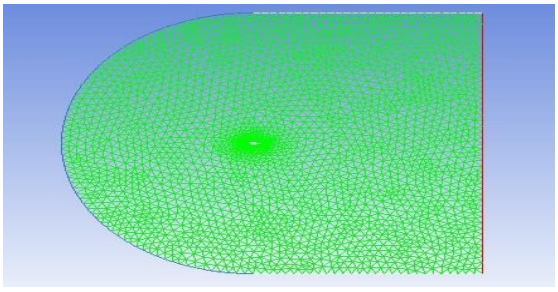

Figure 4-4 NREL S809 meshing by using structured grid

In Figure 4-5, close to the aero foil surface, the most grids should be located near the leading and trailing edges since these are critical areas with the steepest gradients. It is better to transit the mesh size smoothly, because the large and discontinuous transition may decrease the numerical accuracy.

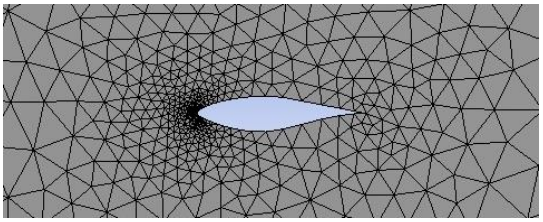

Figure 4-5 Mesh around NREL S809 by using unstructured grid

When the identical mesh strategy was used in unstructured grid: close to the aero foil surface, the most grids should be located near the leading and trailing edges to capture the pressure and velocity gradient, and use coarser mesh in the far-field area.

Velocity inlet and pressure-outlet boundary condition was used in meshing methods the computational domain is large enough. Aero foil is treated as stationary wall condition with no slip shear condition. The computational condition is seen in Table 4-1 for viscous-laminar flow over an aero foil.

4.3 LAMINAR FLOW

Table 4-1 Computational conditions of aero foil simulation

Aero foil	NREL S809
Simulation type	Steady simulation
Fluid material	Air
Temperature	288.16 K
Viscosity	$1.7894e^{-05}$ m^2/s
Outlet pressure	0 Pascal
Density	$1.225kg/m^3$
Wind speed	30m/s
CFD algorithm	Simple
Interpolating scheme	Pressure(standard) Momentum(second order upwind)
Boundary condition	Velocity inlet Pressure outlet Stationary airofoil wall with no slip Stationary wall with specified shear

Simulation was carried out for various angle of attack and lift coefficient, drag coefficient and moment coefficient were calculated.

Table 4-2 Cl, CD and CM for various angle of attack

AOA	C_M	C_L	C_D	C_L/C_D
0	0.0013	0.0209	0.0186	1.123
2	0.002	0.0304	0.06695	0.769
4	0.00268	0.0453	0.0634	0.714
6	0.0031	0.059	0.0583	1.012
8	0.001	0.073	0.051	1.43
10	0.0012	0.0874	0.0429	2.037
12	0.0013	0.10078	0.0329	3.06
14	0.0015	0.1131	0.0217	5.211
16	0.00166	0.124	0.0098	12.65
18	0.0017	0.1344	-0.0092	-14.6
20	0.0019	0.142	-0.0028	-50.7
25	0.002	0.1464	-0.0026	-56.3
26	0.002009	0.1401	-0.0161	-8.7
27	0.0018	0.1288	-0.008	-16.1
28	0.00186	0.1236	-0.007	-17.657
29	0.00176	0.1111	-0.0029	-38.31

Figure 4-6 is the polar curve of the lift coefficient: the horizontal-axis is the value of iteration times and the vertical-axis represents the value of the lift coefficient.

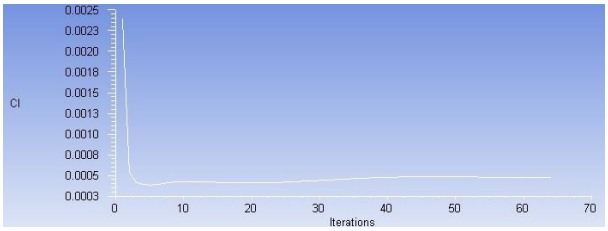

Figure 4-6 The value of lift coefficient for AOA 10^0

The lift coefficient is going down with the increase in number of iteration. Finally the lift coefficient converges after 64 number of iteration. Similarly, figure 3-7 and 3-8 shows the convergence of drag coefficient and moment coefficient for AOA 10^0 .

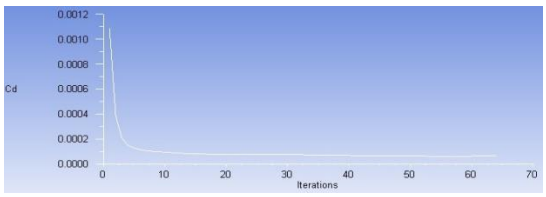

Figure 4-7 The value of Drag coefficient for AOA 10^0

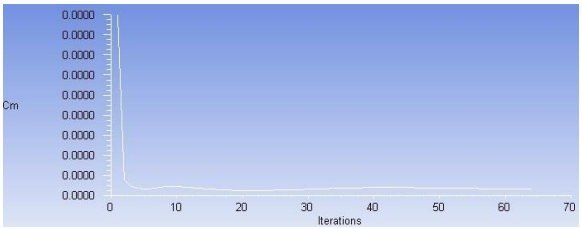

Figure 4-8 The value of Moment coefficient for AOA 10^0

The maximum total pressure on S809 was 653 Pascal, which is located at the leading edge of the airfoil. In the trailing edge the total pressure varies from 132 Pascal to 226 Pascal for AOA 10^0 .

In case of static pressure distribution, the maximum pressure occurs at leading edge with is about 532 Pascal

Figure 4-9 and 4-10 show static and total pressure contour around an aero foil for AOA 10^0 .

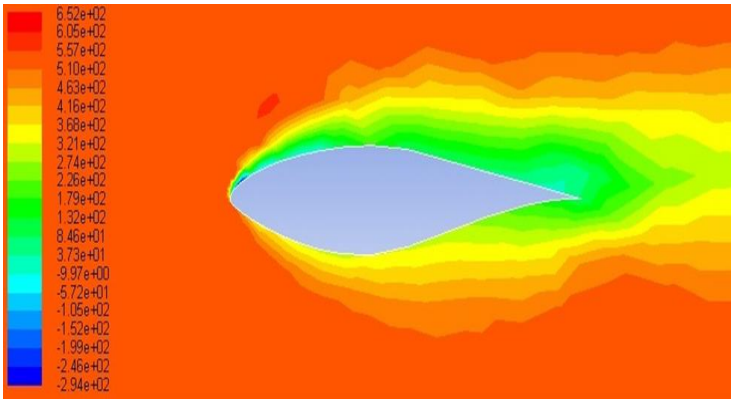

Figure 4-9 Total pressure contour at 10°

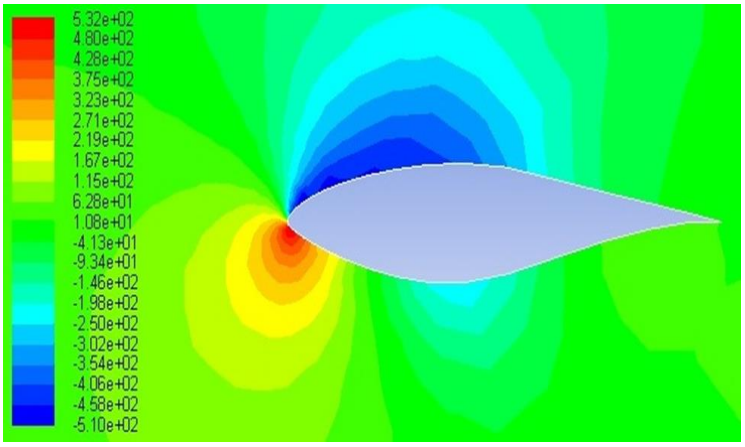

Figure 4-10 Static pressure contour at 10°

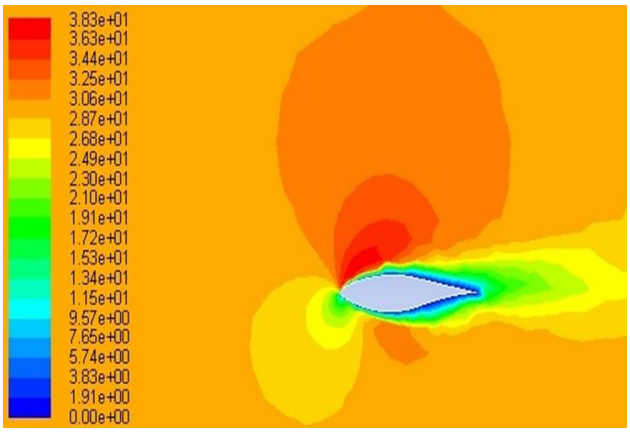

Figure 4-11 Velocity contour at 10°

From figure 4-11, the velocity of air is maximum at leading edge of the airfoil which is about 38.3 m/s and this velocity decreases to about 15.3 m/s at the trailing edge.

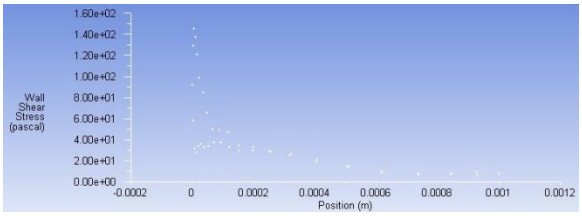

Figure 4-12 wall shear stresses along with position

From fig 4-12, the shear stress becomes zero at position of 0.001 m of aero foil. It is the position where the separation of air from airfoil begins and leads to the stall condition. To find the stall condition, optimum angle of attack is determined. Optimal angle of attack is determined from the following graph plotted between AOA v/s CL.

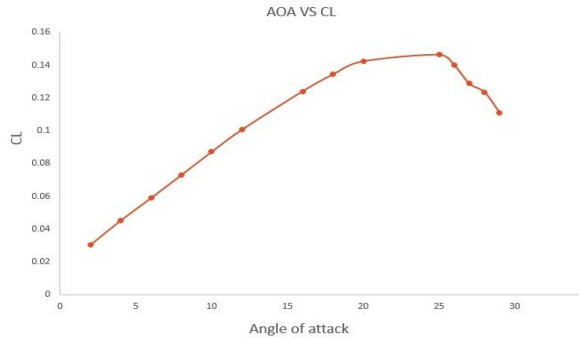

Figure 4-13 AOA VS Cl

From figure 4-13, optimal angle of attack is about 25°.After that the lift coefficient is decreasing. Similarly graph has been plotted in figure 4-13 for CM and CD for various angle of attack.

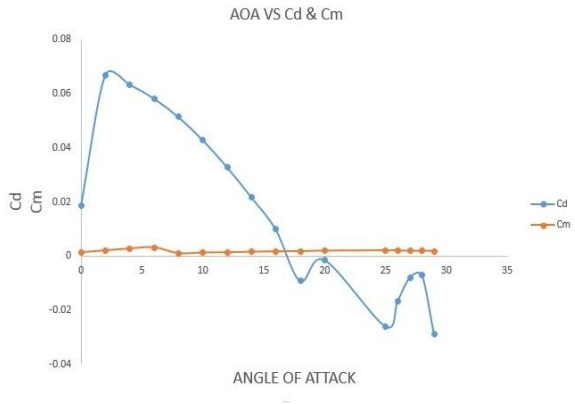

Figure 4-14 AOA vs CD and CM

From above figure, drag coefficient is decreasing with increase in angle of attack. The maximum lift coefficient is 0.066 and the minimum drag coefficient is -0.0029.

4.4 TURBULENT FLOW

Spalart-Allmaras model will be used for turbulent modeling because it is designed specifically for aerospace application, which involves wall-bounded flow and has been shown good results for boundary layers subjected to adverse pressure gradients. Before running the simulation, lift, drag and pitching moment coefficients need to be monitored in ANSYS-Fluent and will be used to estimate the convergence of calculation. Lift coefficient is defined to be perpendicular to the direction of oncoming airflow; drag coefficient is defined to be parallel to the direction of oncoming airflow and the pitching moment center is set at 1/4 chord length from the leading edge.

The computational condition is seen in Table 4-3 for turbulent flow over an aero foil.

Table 4-3 Computational conditions of aero foil simulation

Aero foil	NREL S809
Simulation type	Turbulent
Turbulent model	Spalart-Allamaras
Reynolds number	12500
Density	1.225 kg/m^3
Turbulent viscosity	6.25e-05 m^2/s
Density	1.225 kg/m^3
Outlet pressure	0 Pascal
Wind speed	30 m/s
CFD algorithm	Simple
Interpolating scheme	Pressure(standard) Momentum(Second order Upwind) Modified turbulent viscosity(First order upwind)
Boundary conditions	Velocity inlet Pressure outlet Stationary aero foil wall with no slip Stationary wall with shear

Simulation was carried out for various angle of attack and lift coefficient, drag coefficient and moment coefficient were calculated.

Table 4-4 Cl, CD and CM for various angle of attack

AOA	CM	CL	CD	CL/CD
0	0.00133	0.05	0.0220	2.27
5	0.003	0.0526	0.0663	0.38
10	0.00155	0.088	0.04768	1.84
15	0.0016	0.12	0.0203	5.9
20	0.0019	0.143	-0.0077	-18.57
25	0.00198	0.141	-0.013	-10.84
26	0.00196	0.134	-0.015	-8.9

Figure 4-15 is the polar curve of the lift coefficient: the horizontal-axis is the value of iteration times and the vertical-axis represents the value of the lift coefficient.

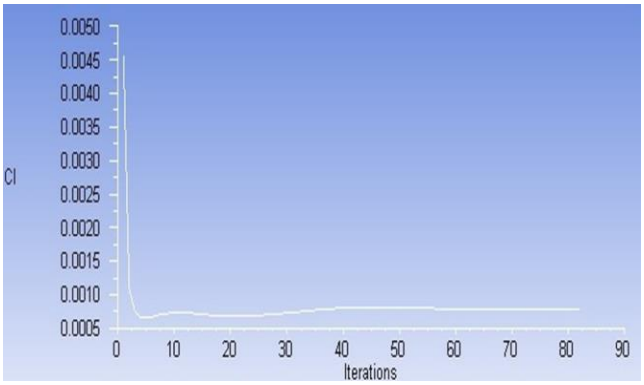

Figure 4-15 lift coefficient for AOA 20^0

The lift coefficient converges after 83 number of iteration and corresponding values of CD and CM are also taken.

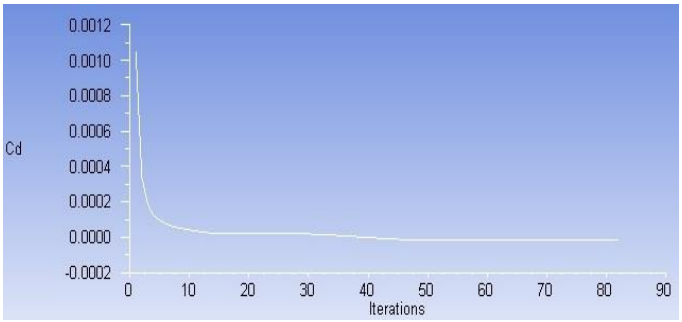

Figure 4-16 Drag coefficients for AOA 20^0

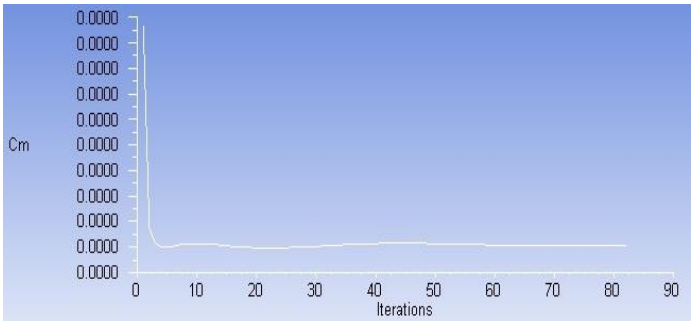

Figure 4-17 Moment coefficients for AOA 20^0

Then the pressure distribution and velocity distribution for an aero foil for turbulent flow was analysed.Figure 4-18,4-19 and 4-20 shows the static pressure, total pressure and velocity counter at 20^0 angle of attack.

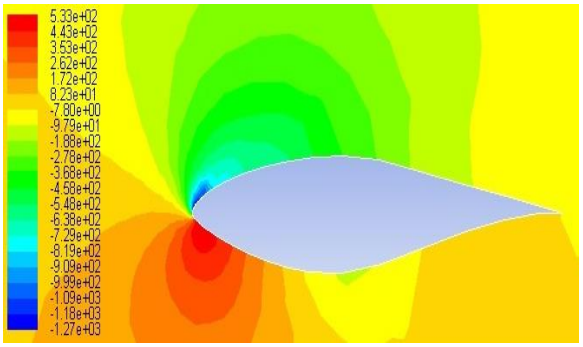

Figure 4-18 Static pressure for AOA 20^0

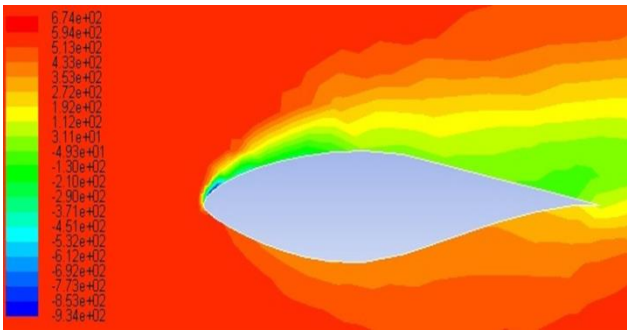

Figure 4-19 Total pressure for AOA 20^0

In figure 4-18 and 4-19, the leading edge has maximum pressure. The maximum static pressure is 67.4 Pascal and maximum total pressure is 53.3 Pascal.

Velocity counter is also shown in figure 4-20.

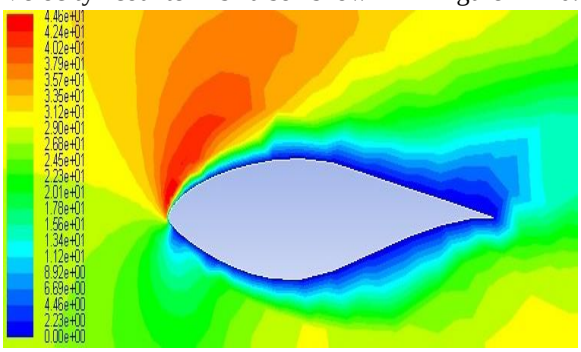

Figure 4-20 velocity contours for AOA 20^0

From above figure, it is analyzed that maximum velocity distribution occurs at the leading edge of the aero foil and is decreases till it reaches the trailing edge.

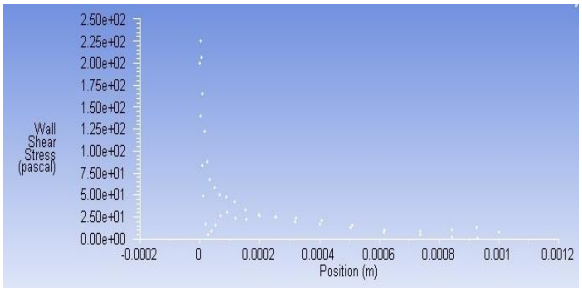

Figure 4-21 Wall shear stress counter for AOA 20^0

From above figure 4-21, wall shear stress is null between position 0.0008m and 0.001m.Therefore the separation of air from airfoil takes place in this region. After that the aero foil goes into stall regime. To find stall regime, optimal angle is determined for turbulent flow also. Following figure 4-22 is used to determine the optimum angle of attack.

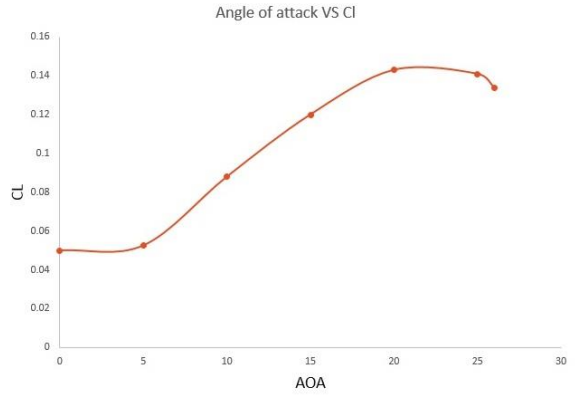

Figure 4-22 AOA vs CL

From above graph optimum angle of attack is in between 20^0 to 25^0 AOA

Similarly, graph has been plotted for CD and CM for various angles of attack.

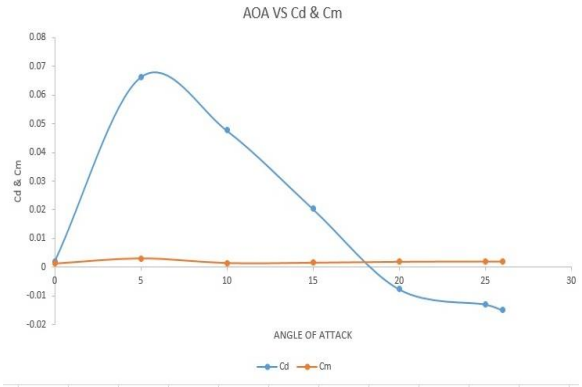

Figure 4-23 AOA vs CD and Cm

The graph is different to laminar flow and the maximum and minimum value of CD and Cm are also different for various angle of attack.

5. RESULTS AND DISCUSSION

In this work has been evaluated the aerodynamic property of horizontal-axis wind turbine blades through two dimensional computational fluid dynamics (CFD) analyses. Here analyzed the aero dynamic property of aero foil like lift, drag and moment at different angle of attack. Similarly analyzed pressure and velocity distribution over an aero foil to determine optimal angle of attack and the separation point.

6. CONCLUSIONS

- CFD analysis shows a good performance in calculating the lift, drag and moment coefficients of aero foils especially for low angles of attack. So this CFD analysis has a good ability to predict the optimum and critical angle of attack.

- Thus, the optimum angle of attack is determined for both laminar and turbulent flow.

- Optimum angle of attack is determined because with the increase in angle of attack wind turbine blade will get into fully stalled regime. When wind turbine blades are working on the stall condition, noise will be increased significantly and wind turbine vibration may happen. This leads the aero foil into fully stalled position so that limits the aerodynamic power output.

7. FUTURE WORK

- Using of structural grid increases the order of accuracy. So aero foil simulation for both laminar and turbulent flow can be done using structural grid.

- Turbulent models have been shown to play an important role in CFD modeling of wind turbines. The next step; in order to simulate the wind turbine wake, a high performance computer should be employed to implement the DES and LES techniques.

- In three-dimensional simulations, different blade and hub geometries can be simulated to evaluate which one has a highest power output. These parameters are of the utmost importance for engineers in order to improve the performance of wind turbine blades.

8. REFERENCES

[1] Chris kaminsky, et al. “A CFD study of Wind Turbine Aerodynamics”, 2012.

[2] Han Cao, “Aerodynamics Analysis of small Axis wind Turbine blades by using 2D and 3D modeling”, May 2011.

[3] Muhammad I.H.B.Z. Abidin, “CFD analysis of miniature Wind Turbine”, 6 December 2011

[4] David Hartwanger, et al, “3D modeling of wind turbine Using CFD”, 11 June 2008

[5] Dayanesh A. Digraskar, “Simulation of flow over Wind Turbines”, 2010

[6] Walter P. Wolfe, Stuart S. Ochs, “CFD Calculations of S809 Aerodynamic Characteristics”

[7] Carlo Enrico Carcangi, “CFD-RANS Study of Horizontal Axis Wind Turbines”, January 2008

[8] World Energy Report 2009. World Wind Energy Association. 9th World Wind Energy Conference & Exhibition Large-Scale Integration of Wind Power. March 2010.

[9] Vaughn Nelson,. 2009. Wind Energy: Renewable Energy and the Environment. New York: CRC Press.

[10] Fluent Inc., 2006, “12.7 Reynolds Stress Model (RSM) Theory” FLUENT 6.3 User’s Guide Fluent Inc.

[11] Chalothorn Thumthae and Tawit Chitsomboon. Optimal Pitch for Untwisted Blade Horizontal Axis Wind Turbine. In: SEE (Sustainable Energy and Environment) 2006, The 2nd Joint International Conference. Bangkok, Thailand. 21-23 November 2006.

[12] Alexandros Makridis and John Chick, 2009, CFD Modeling of the wake interactions of two wind turbines on a Gaussian Hill, EACEW 5 Florence, Italy. 19th-23rd July 2009

[13] Fluent Inc, 2006, “12.3.2 Transport Equation for the Spalart-Allmaras Models Theory” FLUENT 6.3 User’s Guide Fluent Inc.

[14] Fluent Inc, 2006, “12.4 Standard, RNG and Realizable - Models Theory” FLUENT 6.3 User’s Guide Fluent Inc.

